Binding of endostatin to endothelial heparan sulphate shows a differential requirement for specific sulphates

Fiona H. BLACKHALL*, Catherine L. R. MERRY*[1], Malcolm LYON*, Gordon C. JAYSON*, Judah FOLKMAN†, Kashi JAVAHERIAN† and John T. GALLAGHER*

*Department of Medical Oncology, University of Manchester, Cancer Research UK, Christie Hospital NHS Trust, Manchester M20 4BX, U.K., and †Department of Surgery, Children's Hospital, Harvard Medical School, Boston, MA 02115, U.S.A.

Endostatin is a naturally occurring proteolytic fragment of the C-terminal domain of collagen XVIII. It inhibits angiogenesis by a mechanism that appears to involve binding to HS (heparan sulphate). We have examined the molecular interaction between endostatin and HS from micro- and macrovessel endothelial cells. Two discrete panels of oligosaccharides were prepared from metabolically radiolabelled HS, using digestion with either heparinase I or III, and then examined for their endostatin affinity using a sensitive filter-binding assay. Two types of endostatin-binding regions were identified: one comprising sulphated domains of five or more disaccharides in length, enriched in 6-O-sulphate groups, and the other contained long heparinase I-resistant fragments. In the latter case, evidence from the present study suggests that the binding region encompasses a sulphated domain fragment and a transition zone of intermediate sulphation. The contribution to binding of specific O-sulphate groups was determined using selectively desulphated HS species, namely HS from *Hs2st*$^{-/-}$ mutant cells, and by comparing the compositions of endostatin-binding and non-binding oligosaccharides. The results indicate that 6-O-sulphates play a dominant role in site selectivity and 2-O-sulphates are not strictly essential.

Key words: angiogenesis, endostatin, heparin sulphate, oligosaccharide, sulphation.

INTRODUCTION

Heparan sulphate (HS) is an essential co-receptor for several pro-angiogenic growth factors, e.g. FGF-2 (basic fibroblast growth factor 2), VEGF (vascular endothelial growth factor) and HGF/SF (hepatocyte growth factor/scatter factor), which deliver mitogenic and migratory signals to endothelial cells (ECs) [1]. The potential role of HS as a mediator in the balance between pro- and anti-angiogenic signalling is suggested by the observation that HS is also required for the anti-angiogenic effect of factors such as endostatin, a widely studied peptide inhibitor of angiogenesis.

HS is an anionic linear polymer with 50–200 saccharides covalently attached to specific proteins, forming proteoglycans at the cell surface (syndecans, glypicans and CD44 v3-variant) and in the extracellular matrix (perlecan, agrin and collagen XVIII) [2]. The HS chains are synthesized by enzymes that initially polymerize a chain of repeating GlcA and GlcNAc units, which are then variously modified by N- and O-sulphation and uronate epimerization [converting GlcA into IdoA (iduronic acid)] [3]. These modifications occur in clusters, creating polymorphic S-domains (sulphated domains) that form the principal recognition sites for heparin/HS-binding proteins. Flanking the S-domains are regions of alternating N-sulphated and N-acetylated disaccharides, termed 'transition zones' or NA/NS domains, which constitute a boundary between the S-domains and the unmodified GlcA–GlcNAc repeat regions of the chain. The functions of the transition zones and unmodified regions are not well understood, but their presence is a key feature that distinguishes HS from the chemically related polymer heparin. Whereas HS is highly variable in sequence and displays cellular polymorphisms, heparin is highly modified along its entire length and, consequently, does not exhibit a domain structure.

Endostatin was initially detected in conditioned medium from a non-metastatic mouse haemangioendothelioma cell line during a screening for novel anti-angiogenic factors [4]. It inhibits FGF-2-induced EC proliferation [4], promotes EC apoptosis [5] and has potent anti-angiogenic activity in mice bearing experimental tumours [4]. Endostatin also attenuates cell migration [6,7] and regulates branching morphogenesis of renal epithelial cells and the ureteric bud [7]. The precursor of endostatin (20 kDa) is the NC1 module of collagen XVIII, which contains three globular endostatin domains. Collagen XVIII is a member of the multiplexin collagen family, widely expressed in basement membranes, which can be substituted with HS chains [8].

Endostatin was first purified by heparin affinity chromatography [4] and was found to contain a discontinuous sequence of 11 basic residues, all of them being arginine residues, clustered on the protein surface, which are highly conserved between species [9]. Subsequent studies confirmed that mutation of critical arginine residues to alanine residues impaired both heparin affinity and bioactivity [10,11]. Primary and secondary heparin-binding sites within the arginine cluster were identified [10]. Initial studies using heparin oligosaccharides predicted that deca- to dodecasaccharides (dp10–12, where dp represents the degree of polymerization, e.g. dp4 for tetrasaccharide) were required for strong binding across primary and secondary sites, and that both 2-O- and 6-O-sulphate groups were necessary for binding [10]. A critical role for 2-O-sulphation was suggested by a previous study [12] in which inhibition of 2-OST (2-*O*-sulphotransferase) activity in melanoma cells using an antisense

Abbreviations used: 2-OST, 2-*O*-sulphotransferase; EC, endothelial cell; BAEC, bovine aortic EC; dp, degree of polymerization, e.g. dp4 for tetrasaccharide; FBA, filter-binding assay; FGF-2, basic fibroblast growth factor 2; GlcNS, *N*-sulphoglucosamine; HMVEC, human neonatal dermal microvessel EC; HS, heparan sulphate; IdoA, iduronic acid; SAX, strong anion exchange; S-domains, sulphated domains; UA, uronic acid; VEGF, vascular endothelial growth factor.

[1] To whom correspondence should be addressed (e-mail cmerry@picr.man.ac.uk).

strategy significantly impaired binding of their HS to endostatin. Further characterization of the binding site in HS was reported by Kreuger et al. [13], who demonstrated that fragments of pig intestinal HS consisting of two N-sulphated regions separated by at least one N-acetylated disaccharide unit (collectively called SAS domains) bound to endostatin.

The aims of the current investigation were to examine the relevance of these binding characteristics to HS from ECs, the natural target of anti-angiogenic endostatin, and to determine the influence of HS sulphation and domain organization on endostatin recognition.

EXPERIMENTAL

Materials

Recombinant human endostatin monomer was purified from the conditioned medium of stable myeloma transfectants as described previously [14,15]. D-[6-^{3}H]glucosamine hydrochloride (20–45 Ci/nmol) and $Na_2{}^{35}SO_4$ (carrier-free; 1200–1400 Ci/nmol) were obtained from DuPont–New England Nuclear (Stevenage, Herts., U.K.). Heparinases I–III (*Flavobacterium heparinum)* were obtained from Grampian Enzymes (Orkney, U.K.). Chondroitinase ABC (*Proteus vulgaris*) and Pronase were purchased from Sigma (Poole, Dorset, U.K.). Gels and resins used were DEAE–Sephacel (Sigma), Sepharose CL-6B and PD-10 desalting columns containing Sephadex G-25 (Amersham Biosciences, Little Chalfont, Bucks., U.K.), Bio-Gel P10 (fine grade) and Bio-Gel P2 (Bio-Rad Laboratories, Hemel Hempstead, Herts., U.K.) and ProPac PA-1 analytical columns (Dionex, Camberley, Surrey, U.K.). Optiphase 'Hisafe' liquid-scintillation cocktail (added in the ratio 3:1, v/v) was obtained from Fisher Chemicals (Loughborough, Leics., U.K.). Bovine lung heparin was kindly provided by Dr B. Mulloy (National Institute for Biological Standards and Control, South Mimms, Herts., U.K.). Size-defined heparin oligosaccharides were obtained from Iduron (Manchester, U.K.) and pig mucosal HS from Sigma. De- or re-N-acetylated HS (loss of 92 % of N-sulphates), selectively de-2-O-sulphated HS (loss of 83.4 % of 2-O-sulphates) and selectively de-6-O-sulphated HS (loss of 54.8 % of 6-O-sulphates and 9.6 % of 2-O-sulphates) were prepared as described previously [16].

Cell culture and purification of metabolically radiolabelled HS

HMVECs (human neonatal dermal microvessel ECs) were maintained in EC basal medium, supplemented with bovine brain extract, 10 ng/ml human epidermal growth factor, 1 μg/ml cortisol, 10 % (v/v) foetal bovine serum, 50 μg/ml gentamicin and 50 ng/ml amphotericin-B (TCS Biologicals, Buckingham, Bucks., U.K.). BAECs (bovine aortic ECs) were cultured on 0.1 % (w/v) gelatin-coated tissue culture flasks in low-glucose Dulbecco's modified Eagle's medium, supplemented with 100 units/ml penicillin/streptomycin, 50 μg/ml ascorbic acid and 10 % (v/v) donor calf serum. Cell populations were expanded to a minimum of five 175 cm^2 flasks between passages 7 and 9 at 37 °C in humidified air containing 5 % CO_2. Antibiotics were removed for 1 week before radiolabelling. Subconfluent monolayers (approx. 70 % confluency) were metabolically radiolabelled with 10 μCi of [^{3}H]glucosamine hydrochloride/ml and 20 μCi of $Na_2{}^{35}SO_4$/ml medium. Combined medium and cell layers were digested with Pronase as described previously [17], and the Pronase-resistant glycosaminoglycans (i.e. hyaluronan, HS and chondroitin/dermatan sulphate) were resolved on a DEAE–Sephacel column (1 cm × 5 cm) by elution with a linear gradient of 0.15–0.825 M NaCl in 20 mM sodium phosphate buffer (pH 7.4) at a flow rate of 15 ml/h. HS, eluting at approx. 0.5–0.6 M NaCl, was pooled and then desalted on a PD-10 column eluted with water. Residual chondroitin/dermatan sulphate in the HS fraction was digested with 40 m-units of chondroitinase ABC in 50 mM Tris/HCl plus 50 mM NaCl (pH 7.9) for 24 h at 37 °C, and then removed by gel-filtration chromatography on a Sepharose CL-6B column (1.5 cm × 66 cm) eluted with 0.2 M NH_4HCO_3 at a flow rate of 12 ml/h. Fractions of 1 ml were collected, aliquots taken for scintillation counting and fractions corresponding to HS were pooled, freeze-dried and reconstituted with MilliQ water. The residual peptide attached to HS chains was eliminated by treatment with 50 mM NaOH, 1 M $NaBH_4$ at 45 °C for 48 h. HS chains were recovered on a Sepharose CL-6B column as described above and freeze-dried. Metabolically labelled [^{3}H]HS or [^{35}S]HS from 3T3 fibroblasts and primary (both wild-type and *Hs2st*$^{-/-}$ mutant) mouse fibroblasts were prepared as described previously [18,19].

FBA (filter-binding assay)

The FBA [20] was optimized for use with a range of (3–300) × 10^3 c.p.m. of [^{3}H]HS. The HS was incubated with 40 μM endostatin plus any non-radioactive GAG competitor, for 2 h at room temperature (23 °C) in a solution containing 0.13 or 0.05 M NaCl in 10 mM Tris/HCl (pH 7.0). Samples were applied to buffer-equilibrated cellulose nitrate filters (0.2 μm pore size) under a vacuum. Unbound HS was eluted under a vacuum with three 1 ml aliquots of incubation solution. Bound HS was eluted with increasing concentrations of NaCl in 10 mM Tris/HCl (pH 7.0). All fractions, and the filters at the end of the experiment, were monitored for radioactivity by scintillation counting. Binding of [^{3}H]HS to 40 μM endostatin in 0.13 M NaCl and 10 mM Tris/HCl (pH 7.0) approached saturation (approx. 80 % HS bound). The length of incubation, the presence of BSA or the use of a subphysiological NaCl concentration (0.05 M) did not significantly alter the proportion of intact HS that was bound. Further modifications to the technique of Maccarana and Lindahl [20] were made as follows: initial incubation volumes were decreased from 100–200 μl to 25 μl to decrease protein consumption, and the volumes of salt washings used to elute HS were decreased to 3 × 1 ml.

Preparation of HS oligosaccharides

Heparinases III and I were individually used to excise S-domains and heparinase I-resistant oligosaccharides respectively. Intact chains were treated with two additions of enzyme (20 m-units/ml) in 0.1 M sodium acetate plus 0.1 mM calcium acetate (pH 7.0) for a minimum of 18 h at 37 °C. S-domains were size-resolved by Bio-Gel P10 gel-filtration columns (170 cm × 1 cm) eluted with 0.1 M NaCl (pH 8.8). The sizes of heparinase I-resistant oligosaccharides were established by their elution positions, relative to the calibration of Wasteson [21], on a Sepharose CL-6B column (1.5 cm × 66 cm) eluted with 0.2 M NH_4HCO_3 at a flow rate of 12 ml/h.

S-domain profiling and sequencing

S-domains of defined size classes (dp4–12) were fractionated into their component species by SAX (strong anion exchange)-HPLC on a ProPac PA-1 (4.6 mm × 250 mm) column using a range of linear NaCl gradients [18]. Fractions of 0.5 ml were collected, aliquots were taken for scintillation counting and peaks of interest representing single-oligosaccharide species were pooled, desalted on PD-10 columns and freeze-dried. Sequence

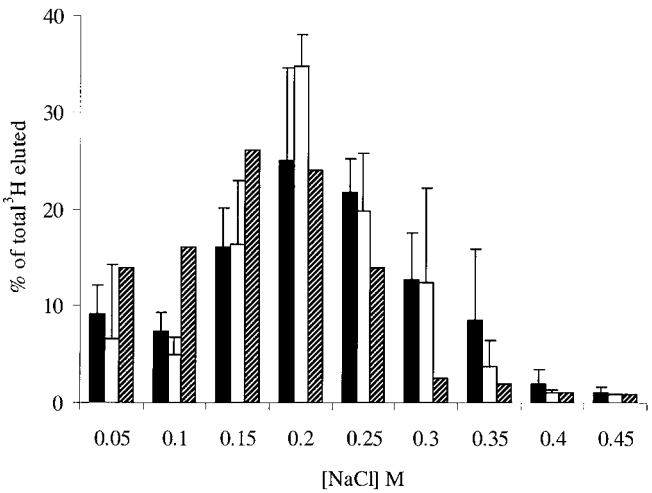

Figure 1 FBA characterization of the binding of endostatin to HS species

HS from HMVECs (solid bars), BAECs (open bars) and 3T3 fibroblasts (hatched bars) was incubated with endostatin in 0.05 M NaCl and 10 mM Tris/HCl (pH 7.0) before application to the FBA. After washing with 0.05 M NaCl, bound chains were eluted with increasing NaCl concentrations. ^{3}H counts are expressed as a percentage of the total ^{3}H eluted. Bars represent means ± S.D. from five independent experiments (for HS from 3T3 fibroblasts, $n = 1$).

analysis was performed using step sequencing as described in [18], or inferred by matching S-domain profiles with previously sequenced oligosaccharides [18].

Disaccharide composition of HS oligosaccharides

HS samples [(3–5) × 10^3 c.p.m. of ^{3}H] in a mixture containing 0.1 M sodium acetate and 0.1 mM calcium acetate (pH 7.0) were treated with either heparinase I (for S-domains) or heparinase III (for heparinase I-resistant domains), followed in both cases by treatment with heparinase II, at 37 °C for 24 h. Disaccharides were resolved by SAX-HPLC on a ProPac PA-1 (4.6 mm × 250 mm) column and identified by referring to known standards [17].

RESULTS

Affinity of endostatin for HS

The FBA [20] was used to compare the relative affinities of various HS oligosaccharides for endostatin. Complexes of endostatin and HS were adsorbed on to nitrocellulose filters from which HS chains were released by washing with increasing concentrations of NaCl. The affinities of HMVEC-, BAEC- and 3T3-derived [^{3}H]HS species for endostatin are compared in Figure 1. [^{3}H]HS recovered by elution with specific NaCl concentrations retained its original elution position on rebinding (results not shown). Most of the bound HS eluted with 0.2–0.25 M NaCl and no significant binding remained above 0.35 M for any HS type.

Interaction of HS and heparin saccharides with endostatin

Heparin oligosaccharides dp4–20 were screened using the FBA to examine their ability to compete with EC [^{3}H]HS for binding to endostatin. The shortest oligosaccharide to show some competition was dp8, although dp10 was the more effective (Figure 2). Sasaki et al. [22] predicted from the crystal structure of

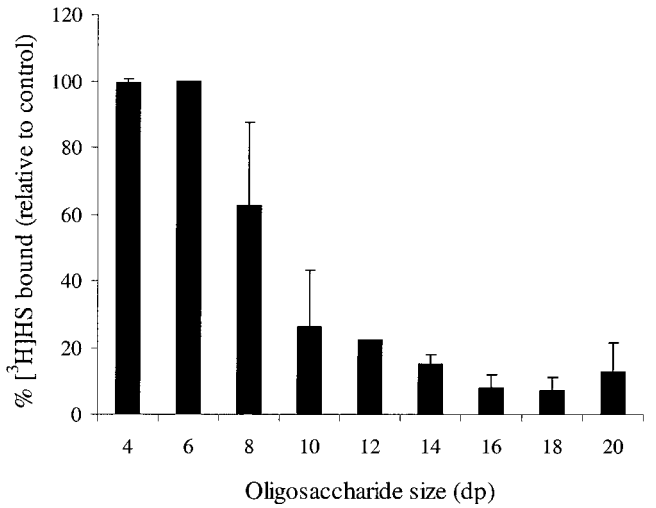

Figure 2 Dependence on oligosaccharide size of the binding of endostatin to heparin oligosaccharides

Heparin saccharides (dp4–20) were assayed for their ability to inhibit the binding of HMVEC-derived [^{3}H]HS to endostatin in 0.13 M NaCl and 10 mM Tris/HCl (pH 7). After washing with 0.13 M NaCl, the bound material was eluted with three 1 ml aliquots of 0.1 M NaCl. Bound [^{3}H] is expressed as a percentage of that bound in the absence of competing oligosaccharides.

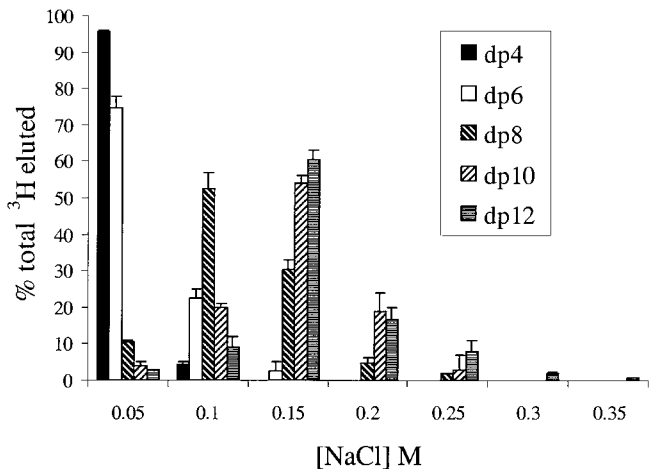

Figure 3 Binding of HS oligosaccharides to endostatin

Size-defined HS oligosaccharides (S-domains, dp4–12) from HMVEC-derived [^{3}H]HS were assayed for direct binding to endostatin using the FBA as described in the legend to Figure 1. ^{3}H counts are expressed as a percentage of the total ^{3}H eluted.

endostatin that highly sulphated dp4–6 could be accommodated in the primary heparin-binding site, with a longer oligosaccharide (dp10/12) required to extend into the secondary binding site. Our findings suggest that interaction across both the primary and secondary sites (by at least a dp10) is necessary for an effective inhibition of the binding of endostatin to polymeric HS. Both sites may therefore need to be engaged to give measurable affinity at physiological salt concentrations. However, a question arose as to whether short oligosaccharides from endothelial HS could bind to endostatin, perhaps by sole recognition of the proposed primary binding site, in low-ionic-strength solution (50 mM NaCl plus 10 mM Tris/HCl, pH 7.0). To address this, heparinase III-excised S-domains of defined size (dp4–12) were purified from HMVEC-derived [^{3}H]HS, and their disaccharide compositions (see below) and endostatin-binding characteristics (Figure 3) were assayed.

No binding was observed for dp2s (results not shown) or dp4s, but a fraction of the dp6s bound with weak affinity. Longer S-domains of ⩾dp10 bound to endostatin with apparent affinities approaching that of the intact chains (see Figures 1 and 3).

Sequence analysis of minimal binding hexasaccharides

S-domain profiling of EC HS by SAX-HPLC indicated the presence of four species of dp6 S-domain (dp6a–d) that had previously been characterized from 3T3 HS [18] (Figures 4A–4C). To determine the relative affinities of dp6a–d for endostatin, we first performed a preparative FBA in which approx. 5×10^4 c.p.m. of ^{3}H-labelled dp6 S-domains from HMVEC-derived HS were incubated with endostatin in 50 mM NaCl. Bound dp6 were eluted with 3 × 1 ml of 0.1 M NaCl plus 10 mM Tris/HCl (pH 7.0). Bound and unbound fractions were monitored by scintillation counting, desalted and then subjected to S-domain profiling by SAX-HPLC and total disaccharide compositional analysis. In the bound pool, the S-domain profiles demonstrated a clear selection for dp6d (Figure 4E), whereas dp6a and dp6b eluted with the non-binding fraction (Figure 4D). It was difficult to study the behaviour of dp6c due to its low overall abundance. The disaccharide compositions of the binding and non-binding pools are shown in Table 1. The quantity of trisulphated disaccharide UA(2*S*)-GlcNS(6*S*) (where UA stands for uronic acid and GlcNS for *N*-sulphoglucosamine) is significantly increased in the binding pool. Taking account of the disaccharide compositions of the binding and non-binding saccharides, combined with their elution positions on SAX-HPLC [25], the sequences of the saccharides were consistent with:

ΔUA-GlcNS-IdoA(2*S*)-GlcNS-IdoA-GlcNAc (6a)

ΔUA-GlcNS-IdoA(2*S*)-GlcNS-GlcA-GlcNAc (6b)

ΔUA-GlcNS-IdoA(2*S*)-GlcNS-IdoA(2*S*)-GlcNAc (6c)

ΔUA-GlcNS-IdoA(2*S*)-GlcNS(6*S*)-IdoA-GlcNAc (6d)

The major HMVEC-HS dp6 S-domain with affinity for endostatin is 6d. However, the presence of minor quantities of UA-GlcNS(6*S*) and UA-GlcNAc(6*S*) in the disaccharide composition of the bound HMVEC dp6s suggests co-elution of additional minor species. Oligosaccharides 6c and 6d are isomers with identical degrees of sulphation (two N- and two O-sulphates). In 6c, there is a 2-O-sulphate on the reducing terminal N-acetylated disaccharide, whereas in 6d there is a 6-O-sulphate group on the central GlcNS. To establish accurately the relative abilities of these sequences to bind to endostatin, BAEC dp6a–d were individually purified and tested (Figure 5). This demonstrated an interaction with both dp6c and dp6d with >40% of the total counts eluted for each of these species eluting with 0.1 M NaCl. For all species (dp6a–d), the fraction eluting at 0.15 M NaCl was <2%.

Affinity fractionation and structural characterization of dp8 and dp12 S-domains

Using a strategy similar to that described above for dp6 species, a mixed population of dp8 S-domains were incubated with endostatin and fractionated using a preparative FBA into species that eluted with 0.05, 0.1 or 0.15 M NaCl (all in 10 mM Tris/HCl, pH 7.0) respectively. S-domain profiling demonstrated that, although there is a larger variety of dp8 S-domains when compared with dp6 S-domains, they could still be affinity-fractionated into pools of predominantly non-overlapping species (Figure 6). S-domains of ⩾dp10 from HMVEC HS bound to endostatin with affinity equivalent to that of dp12 S-domains from 3T3 fibroblasts. The latter were incubated with endostatin and subfractionated into unbound (eluted with 0.05 M NaCl), low-affinity (0.1 M NaCl), medium-affinity (0.15 M NaCl) and high-affinity (0.3 M NaCl) pools. After rebinding, each pool reproduced its original elution position (results not shown). Analysis of the disaccharide compositions of each binding pool for dp8s and dp12s (Table 1) demonstrated that increased sulphate content confers stronger binding on these S-domains. The presence of multiple 6-O-sulphates in the medium- and highest-affinity dp12s distinguishes them from the non-binding domains and low-affinity-binding dp12 S-domains, which have on average less than one 6-O-sulphate group/oligosaccharide. The trisulphated

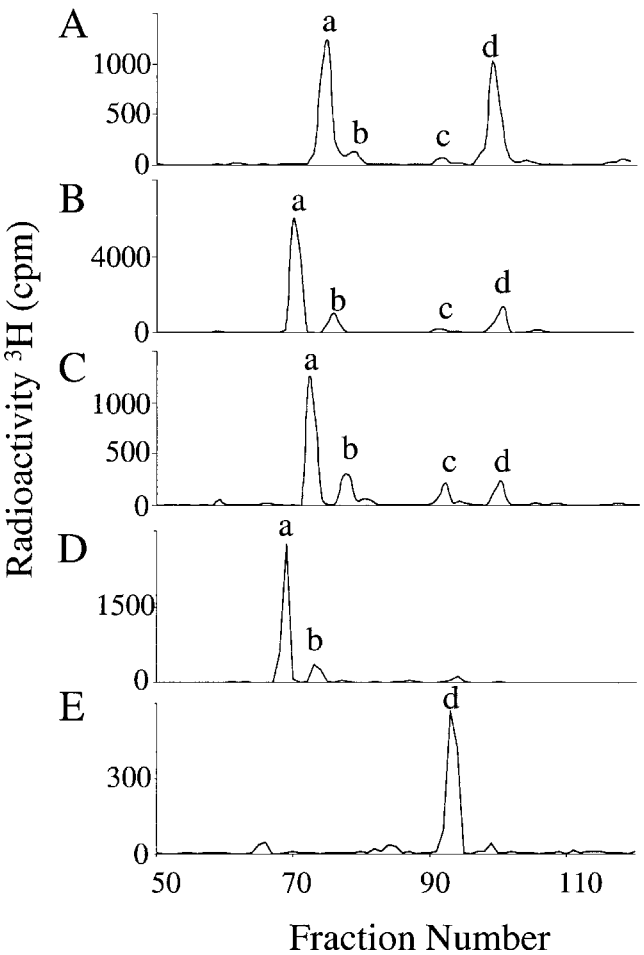

Figure 4 S-domain profiling of EC HS

dp6 S-domains (peaks a–d) from HMVEC (**A**), BAEC (**B**) and 3T3 fibroblast (**C**) HS species were separated by SAX-HPLC using a linear gradient of 0–1 M NaCl for 80 min at 1 ml/min. Fractions of 1 ml were monitored by scintillation counting. The drift in elution position of the S-domains between runs was due to differences between columns and HPLC systems. Peak identities were checked by comparison of elution positions with sequenced 3T3 fibroblast and BAEC-derived dp6 S-domains and by disaccharide analysis (see the Sequence analysis of minimal binding hexasaccharides subsection for the sequences of 6a–d). dp6 S-domains bound to endostatin, as described in the legend to Figure 1, were separated according to their affinity. Unbound material was eluted with three 1 ml aliquots of 0.05 M NaCl, whereas bound material was eluted with three 1 ml aliquots of 0.1 M NaCl. After desalting, these pools were analysed by SAX-HPLC, as described above. The non-binding (**D**) and binding (**E**) pools are shown.

Table 1 Disaccharide analysis of endostatin-binding HS oligosaccharides

S-domains from either HMVEC HS (dp6 and dp8) or 3T3 fibroblast HS (dp12) were incubated with endostatin and subfractionated into pools of varying affinity using the FBA. The disaccharide composition of each of these fractions was then assessed by heparinase digestion and SAX-HPLC separation.

	[NaCl] to elute bound dp6 (M)		[NaCl] to elute bound dp8 (M)			[NaCl] to elute bound dp12 (M)			
	0.05	0.1	0.05	0.1	0.15	0.05	0.1	0.15	0.2
Disaccharide structure	Total disaccharides (%)								
UA-GlcNAc	31	26	45	27	20	22	20	17	30
UA-GlcNS	33	32	26	30	21	20	14	11	9
UA-GlcNAc(6*S*)		5		5	6				
UA(2*S*)-GlcNAc		2							
UA-GlcNS(6*S*)				2	3				
UA(2*S*)-GlcNS	34	8	20	23	22	54	51	32	13
UA(2*S*)-GlcNS(6*S*)	2	27	8	12	28	4	15	40	48
Sulphate modification	Number of sulphate groups/oligosaccharide								
N-sulphate	2.1	2.0	2.2	2.7	3.0	4.7	4.8	5.0	4.2
2-O-sulphate	1.1	1.1	1.1	1.4	2.0	3.5	4.0	4.3	3.7
6-O-sulphate	0.1	1.0	0.3	0.8	1.5	0.2	0.9	2.4	2.9
Total sulphates	3.2	4.1	3.6	4.8	6.4	8.4	9.7	11.7	10.7

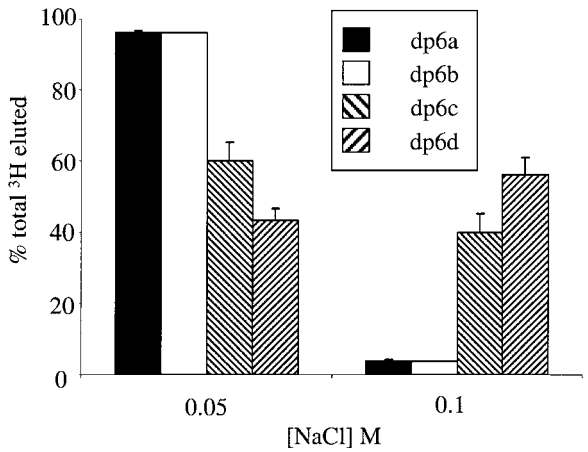

Figure 5 Binding of isolated dp6 S-domains to endostatin

dp6a–d (as shown in Figure 4) were assayed to examine their ability to bind endostatin using the FBA as described in the legend to Figure 1. ^{3}H counts are expressed as a percentage of the total ^{3}H eluted.

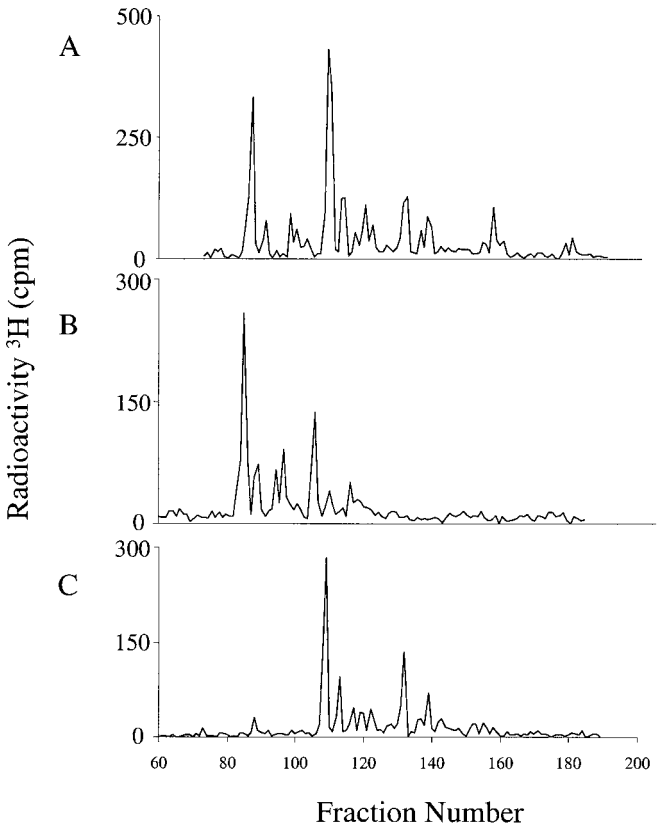

Figure 6 Binding of dp8 S-domains to endostatin

[^{3}H]dp8 S-domains from HMVEC HS were separated by SAX-HPLC using a linear gradient of 0–1.2 M NaCl for 90 min at 1 ml/min (**A**). Fractions of 1 ml were monitored by scintillation counting. The dp8 pool was incubated with endostatin in 0.05 M NaCl and 10 mM Tris/HCl (pH 7) and affinity-fractionated using the FBA. Unbound material was eluted with 0.05 M NaCl (results not shown). Bound material eluted with 0.1 M NaCl (low-affinity pool) and 0.15 M NaCl (high-affinity pool) were re-analysed by SAX-HPLC (**B** and **C** respectively).

disaccharide UA(2*S*)-GlcNS(6*S*) provides most of the 6-O-sulphates in the binding dp8 S-domains and all of them in the corresponding dp12s. It is not possible to discern whether both the 2-O- and 6-O-sulphates present on this disaccharide are of equal importance. However, in contrast with the marked differences in 6-O-sulphate between low- and high-affinity species, there are similar (near maximal) 2-O-sulphate levels in all the dp12 fractions, suggesting that it is specifically the 6-O-sulphate groups present in trisulphated disaccharides that confer stronger binding to these longer S-domains.

Binding characteristics of *Hs2st*$^{-/-}$ mutant HS

The HS 2-OST gene-trap mouse (*Hs2st*$^{-/-}$) synthesizes HS with a characteristic domain structure that is completely deficient in 2-O-sulphate groups, but with significantly increased levels of 6-O-sulphation and a less increased level of N-sulphation [19]. The affinity of [^{3}H]HS from *Hs2st*$^{-/-}$ mouse fibroblasts for endostatin was compared with that of HS from wild-type cells using the FBA. There was no detectable difference in affinity (Figure 7), demonstrating that 2-O-sulphation is not essential for binding.

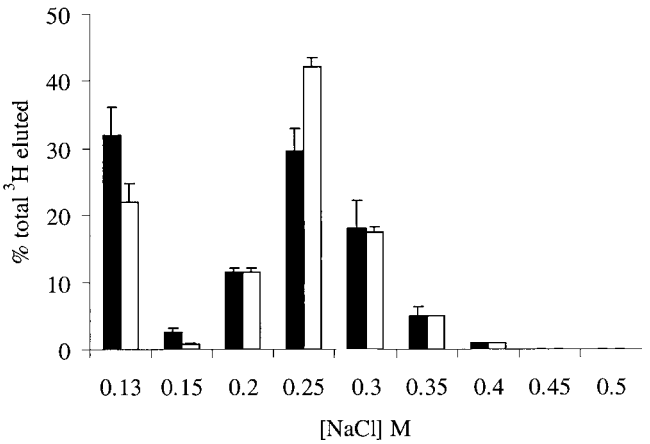

Figure 7 Binding of 2-O-sulphate-deficient HS to endostatin

[^{3}H]HS, produced by primary embryonic fibroblasts extracted from either wild-type or *Hs2st*$^{-/-}$ mice, was assayed to examine its ability to bind to endostatin using the FBA as described in the legend to Figure 2. After washing with 0.13 M NaCl, bound chains were eluted with increasing NaCl concentrations. The ^{3}H counts eluted at each NaCl step for wild-type HS (solid bars) and *Hs2st*$^{-/-}$ HS (open bars) are expressed as a percentage of the total ^{3}H eluted.

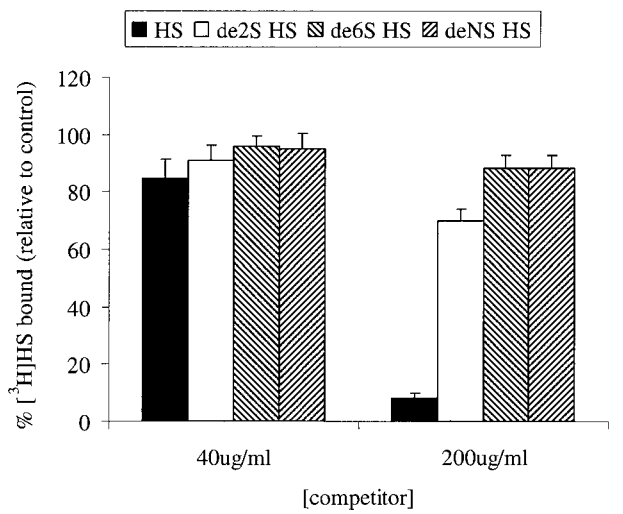

Figure 8 Role of specific sulphate groups in the binding of HS to endostatin

Selectively desulphated HS preparations (at either 40 or 200 μg/ml) were assayed for their ability to inhibit the interaction of HMVEC-derived [^{3}H]HS with endostatin using the FBA as described in the legend to Figure 2. [^{3}H]HS is expressed as a percentage of that bound in the absence of any competing HS species.

Role of specific sulphate groups in the endostatin-binding domain of HS

To examine further the role of specific sulphate groups in the binding of HS to endostatin, competitive binding studies were performed using a range of chemically desulphated HS species (Figure 8). Pig mucosal HS contains an average of 0.85 sulphate groups/disaccharide [16]; half of them are N-sulphates (0.43 per disaccharide) with similar numbers of 2-O- and 6-O-sulphates (0.20 and 0.22 per disaccharide respectively). De-N-sulphation (92% complete) almost completely abolished the competitive binding ability of this HS against intact HMVEC-derived HS. The effects of de-2-O-sulphation (83% complete) were only slightly less marked. An intriguing observation was that the loss

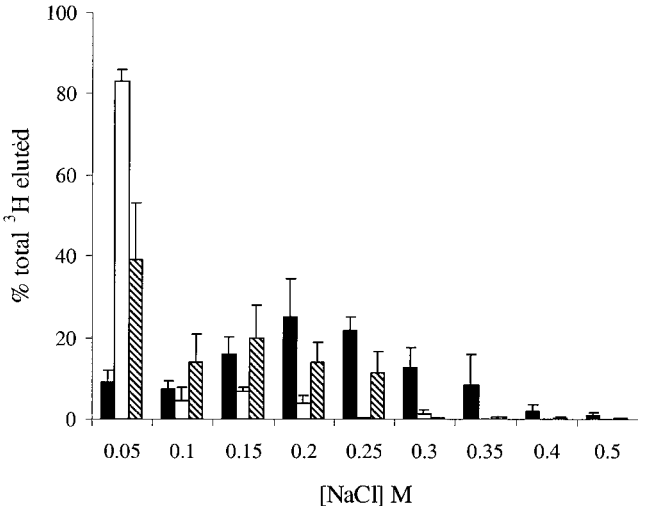

Figure 9 Effect of heparinase digestion on the binding of HS to endostatin

HMVEC-derived [^{3}H]HS was digested with either heparinase I or III. Intact or digested HS was assayed for endostatin binding using the FBA. After washing with 0.05 M NaCl, bound chains were eluted with increasing NaCl concentrations. The ^{3}H counts eluted at each NaCl step for intact (solid bars; $n = 5$), heparinase III-digested (open bars; $n = 3$) and heparinase I-digested (hatched bars; $n = 4$) HS species are expressed as a percentage of the total ^{3}H eluted.

of only 56% of the 6-O-sulphates, which decreased the overall HS sulphation by only 18%, virtually abolished competitive binding. The effect was as dramatic as with near-complete de-N-sulphation, in which there was a much higher (46%) overall decrease in total sulphation. These findings, together with structural data on the endostatin-binding S-domains, suggest that the endostatin interaction with HS is complex and involves the recognition of sulphates at the N-, 2- and 6-positions. However, the binding of endostatin to HS from the *Hs2st*$^{-/-}$ mutant cells demonstrated that 2-O-sulphation is not essential. It is possible that the increased concentration of 6-O-sulphate groups within the N-sulphated regions of the mutant HS from the *Hs2st*$^{-/-}$ mutant cells can compensate for the loss of 2-O-sulphates [19]. Additionally, the unexpected sensitivity of the binding reaction to the removal of only a fraction of the 6-O-sulphates indicates that this substituent may be a key mediator of the binding of endostatin to HS.

Affinity fractionation and structural analysis of heparinase I-excised oligosaccharides

Heparinase I cleaves at IdoA(2*S*) residues in the most sulphated regions of the HS chain. This disrupts the longer S-domains and leaves fragments of S-domains contiguous with transition zones of alternating GlcNAc/GlcNS disaccharides that are in turn attached to intervening N-acetylated domains. Heparinase I-resistant fragments have features in common with the SAS domains chemically derived from pig intestinal mucosal HS, which were shown by Kreuger et al. [13] to bind to endostatin and to inhibit its activity. Similar to the longer S-domains (Figure 3), heparinase I-excised oligosaccharides from HMVEC HS bound to endostatin with a binding strength equivalent to that of the intact HS chains (i.e. elution with 0.2–0.25 M NaCl; Figure 9). They retained their elution positions after rebinding (results not shown). Oligosaccharides in each binding pool (0.05, 0.1, 0.15, 0.2 and 0.3 M NaCl) were recovered for size determination by Sepharose CL-6B chromatography and

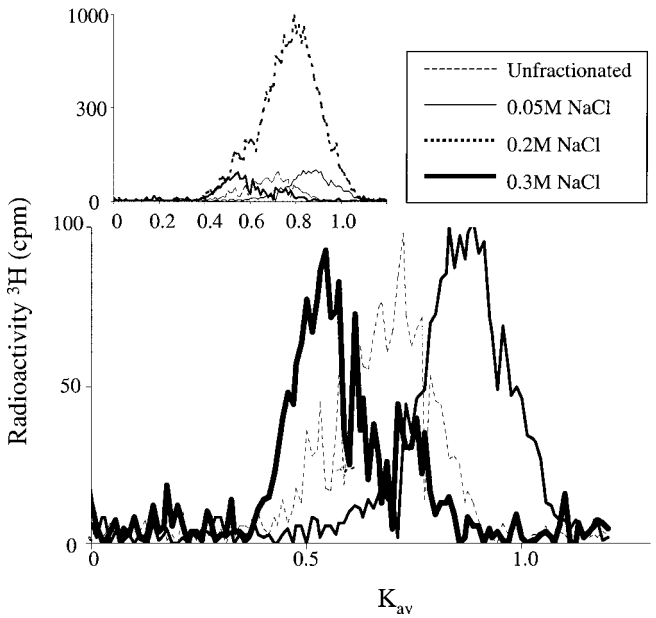

Figure 10 Size fractionation of heparinase I-digested HS fractions with differing affinities for endostatin

A preparative FBA was used to generate pools of heparinase I-digested [^{3}H]HS (from HMVECs) with high (0.3 M NaCl required for elution), medium (0.2 M NaCl) and low (0.05 M NaCl) affinities for endostatin. Their molecular-mass distributions were analysed by size-exclusion chromatography on a Sepharose CL-6B column (1.5 cm × 66 cm) eluted with 0.2 M NH_4HCO_3 at a flow rate of 12 ml/h. Fractions of 1 ml were collected for scintillation counting. Void and total volumes were determined using Blue Dextran and sodium dichromate respectively. The inset shows the unfractionated and fractionated pools for comparison.

analysis of disaccharide composition. The size of the heparinase I-resistant oligosaccharides increased with higher affinity for endostatin, and the strongest binding fragments (eluted with 0.2 and 0.3 M NaCl) ranged from approx. 18–30 disaccharides in length (Figure 10). In contrast with the heparinase III-excised S-domains (Table 1), the highest affinity heparinase I-excised oligosaccharides (Table 2) are predominantly composed of non-sulphated disaccharides with only 36–42 % of the total disaccharides being N- and/or O-sulphated. The small proportion of 2-O-sulphated disaccharides present (approx. 10 %) is due to the substrate specificity of heparinase I [23], which acts at the GlcNS(+/−6*S*)-IdoA(2*S*) linkage. Heparinase I thus acts centrally in IdoA(2*S*)-containing S-domains, and it releases long fragments predominantly composed of unmodified domains and transition zones with S-domain remnants at both ends. Probably, IdoA(2*S*) can occur only as the non-reducing terminal saccharide of most fragments. The disaccharide UA-GlcNAc(6*S*) is believed to reside in the transition zones that flank the S-domains and is present in the excised oligosaccharides at a low frequency. To characterize the arrangement of sulphated disaccharides within the heparinase I-excised oligosaccharides, they were digested with heparinase III and analysed by Bio-Gel P10 gel filtration (results not shown). Most of the linkages were susceptible to heparinase III (87 ± 3 %, $n = 3$), as indicated by absolute yields of 78 ± 5 % dp2, 11 ± 1.7 % dp4 and 10.3 ± 4 % dp6 products. The heparinase III-resistant dp4–6s may correspond to the S-domain remnants or short internal S-domains that resisted heparinase I action [24,25]. Interestingly, nitrous acid depolymerization of the heparinase I-excised oligosaccharides completely abolished binding to endostatin, indicating that the internal repeating sequences of N-acetylated disaccharides are not capable of binding in isolation.

Table 2 Disaccharide composition of endostatin-binding heparinase I-digested HS fragments

Heparinase I-resistant fragments from HMVEC HS were incubated with endostatin and subfractionated into pools of various affinities using the FBA. The disaccharide composition of each of these fractions was then assessed by heparinase digestion and SAX-HPLC. Results are shown for the two highest affinity pools.

	Total disaccharides (%) (means ± S.D.)	
Disaccharide structure	0.2 M NaCl	0.3 M NaCl
UA-GlcNAc	58.0 ± 1	64.0 ± 1
UA-GlcNS	26.0 ± 2	31.0 ± 1
UA-GlcNAc(6*S*)	4.4 ± 0.6	3.2 ± 0.2
UA(2*S*)-GlcNAc	1.8 ± 0	1.9 ± 0.2
UA-GlcNS(6*S*)	0.4 ± 0.6	0 ± 0
US(2*S*)-GlcNS	6.2 ± 3	5.9 ± 0.2
UA(2*S*)-GlcNS(6*S*)	2.4 ± 0	2.4 ± 0.4

Therefore the binding of heparinase I-resistant oligosaccharides to endostatin must be mediated by the arrangement of sulphated residues in the terminal S-domain remnants and their associated transition zones of alternating N-acetylated/N-sulphated disaccharides [26]. This would satisfy the requirement for a sulphated sequence of 10–12 saccharides in length.

DISCUSSION

We have investigated the molecular interaction between endostatin and naturally occurring EC HS using a sensitive FBA. The affinity of endostatin for HS is modest. It is similar for both the HMVEC and BAEC HS species examined in the present study, and equivalent to the affinity of endostatin for fibroblast HS (the present study) and for HS from other sources including pig mucosa, kidney and aorta [10]. We observed that structural motifs within the S-domains, as well as those extending across the boundary between the S-domains and transition zones, bound to endostatin. Heparinase III-excised S-domains of dp6 in length are the smallest oligosaccharides with measurable affinity for endostatin. Longer oligosaccharides enriched in the trisulphated disaccharide UA(2*S*)-GlcNS(6*S*) exhibit progressively stronger binding, with dp10–12s approaching that of intact HS chains. The affinity of 2-O-sulphate-deficient HS from *Hs2st*$^{-/-}$ cells for endostatin was unchanged from that of *Hs2st*$^{+/+}$ cells, indicating that 2-O-sulphate groups are not essential components of the binding site. These binding characteristics distinguish endostatin from FGF-1 and -2, which preferentially recognize sequences confined to long S-domains that are enriched in 2-O-sulphate groups [16,27]. The present findings are consistent with the view that dp10–12 are necessary for effective binding to endostatin [10]. To date, not even a single 'optimal' oligosaccharide for binding to endostatin has been reported. Notably, heparin dp10–12 [10], highly sulphated HS oligosaccharides of dp10–12, and SAS domains with an internal N-acetylated disaccharide [13] have equivalent affinities for endostatin. In the present study, we also demonstrate equivalent affinities of endostatin for highly sulphated S-domains of HS and for enzymically derived oligosaccharides, comprising fragments of S-domains separated by transition zones and N-acetylated repeat regions.

The absence of a 'discrete' binding epitope for endostatin raises the possibility that binding is mediated by 'charge' alone. Compositional analysis of the binding of endostatin to S-domains from HS showed a positive correlation between increased sulphate content and stronger binding for each size-defined

oligosaccharide class. Binding and non-binding subpopulations were predominantly non-overlapping in charge, and the strongest endostatin binding was associated with the most modified sequences that contained the highest proportion of 6-O-sulphates in the trisulphated disaccharide UA(2*S*)-GlcNS(6*S*). However, a higher charge density in a longer sequence did not automatically confer stronger binding (see [NaCl] to elute bound dp12 in Table 1). Therefore this implies some requirement for sulphate groups in specific positions.

The ability of heparinase I-excised oligosaccharides to bind to endostatin strengthens the argument against a purely charge-driven interaction. These oligosaccharides, comprising S-domain remnants and adjacent transition zones of alternating N-acetylated and N-sulphated disaccharides, have a lower charge-to-mass ratio than isolated S-domains. They share many characteristics with the SAS domains that were recently shown to bind to endostatin and modulate the biological activity of ES in a VEGF migration assay [13]. In agreement with this study [13], our results suggest that one or more N-acetylated disaccharides can be accommodated in the endostatin-binding site of HS. The N-acetyl-rich segments are not enough in themselves to mediate binding, suggesting the role of the short S-domain remnants and the adjacent transition zones. However, we have demonstrated that highly sulphated dp4s do not bind endostatin in solution and hexasaccharides only bind with weak apparent affinity (Figure 3). Thus the N-acetylated repeat regions and the adjacent transition zones within the heparinase I-excised oligosaccharides may play a critical role in conferring conformational stability and reactivity on these short-sulphated epitopes. Importantly, the proposition of a combined S-domain/transition-zone binding site satisfies the length and sulphation requirements for optimal interaction of HS with endostatin.

We provide the first direct evidence that binding between HS and endostatin is not strictly dependent on the presence of 2-O-sulphate groups (Figure 7). It is therefore unlikely that the defect in ureteric bud development in the *Hs2st*$^{-/-}$ mouse is due to impaired endostatin function caused by a loss of 'binding' to HS, as has been suggested previously [12]. The role of 2-O-sulphation in endostatin binding is in marked contrast with FGF-2 [27]. Interestingly, fully N-sulphated pig intestinal mucosal dp10–12s with a high affinity for FGF-2, due to the presence of 2-O-sulphate groups, do not bind strongly to endostatin [13]. The role of 2-O-sulphate in the interaction of HS with endostatin is intriguing. In most HS species, this modification clearly plays a role in binding (see Figure 8; results show a marked decrease in ability to compete after 2-O-desulphation), but a complete absence of 2-O-sulphation due to mutation of *Hs2st* has no effect. However, endostatin was found to bind with significantly decreased affinity for HS synthesized by melanoma cells, in which 2-OST activity was inhibited by an antisense strategy [12]. These apparently conflicting results may be due to a compensatory increase in 6-O-sulphation within the N-sulphated regions of HS produced by *Hs2st*$^{-/-}$ cells, which does not occur in HS synthesized by antisense-inhibited cells. Therefore the latter HS may be more akin to chemically 2-O-desulphated HS, in which 6-O-sulphate levels are unchanged. It has been noted, for the interaction between the Hep 2 domain of fibronectin and HS, that 2-O-sulphate groups are more important than 6-O-sulphates, provided that a critical threshold of total sulphation (N-, 2-O- and 6-O-) is exceeded [16]. A similar condition may apply to endostatin, except that once a sulphation 'threshold' is exceeded, 6-O-sulphates are more effective than 2-O-sulphates in the mediation of specific binding. This model is reinforced by our finding that chemical depletion of only 56% of the 6-O-sulphate groups of HS virtually eliminates endostatin binding activity.

Our findings are compatible with the hypothesis that the balance between overall charge versus the involvement of specific structural groups may not be equal for the putative primary and secondary binding sites. In theory, one site may bind to endostatin according to overall charge, possibly to enable initial 'docking' to an HS chain. The other site may then engage a sulphated oligosaccharide of appropriate length, with a requirement for a specific modification, such as a 6-O-sulphate group, in a precise position. If we assume that HS hexasaccharides engage endostatin by its primary site, this could explain why hexasaccharides 6c and 6d bind with similar affinities. Although 6c does not have any 6-O-sulphate group, it has the same overall sulphate content as 6d (see the Results section). However, mutations of Arg^{193}/Arg^{194} to Ala in the secondary binding site are known to decrease the affinity for HS rather than that for heparin [10]. Thus the secondary binding site may have a specific requirement for a precisely positioned 6-O-sulphated disaccharide in HS, whereas the primary binding site may have less stringent requirements.

Endostatin inhibits FGF-2-induced angiogenesis [28]. However, as suggested by our own findings and the previously published results of others [13], the epitopes within HS that bind to FGF-2 and endostatin are distinct. Both heparin dp12s and HS-derived SAS domains in solution can compete with cell-surface HS for binding to endostatin, and they can promote the endostatin-mediated inhibition of VEGF and FGF-2 bioactivity [10,13]. However, the fine structure(s) of bioactive oligosaccharides that promotes the anti-angiogenic activity of endostatin has not been defined. In a mode similar to the requirement for 2-O-sulphation for high-affinity binding of HS to FGF-2, but with 6-O-sulphation necessary for integration into a trimolecular FGF-2/FGFR/HS signalling assembly (where FGFR stands for FGF receptor) [29], endostatin may have different requirements within HS for binding and activation. Although there is accumulating evidence that endostatin does not compete with HS-binding sites for FGF-2 [13], our results cannot exclude a mechanism whereby endostatin antagonizes FGF-2-mediated angiogenesis by binding to 6-O-sulphate groups engaged in the formation of trimolecular FGF-2/FGFR/HS signalling assemblies.

In summary, structural motifs of dp10–12 in length, either within the S-domains of HS or extending across the boundary between the S-domains and transition zones, bind to endostatin. Our results reveal that 2-O-sulphate groups are not essential for this interaction, and suggest novel possibilities for the specificity of this interaction. Binding of endostatin to HS is partly driven by the overall charge, but is also highly dependent on the distinctive arrangement of 6-O-sulphated disaccharide units within the binding sequence.

We thank Professor Lindahl and Dr Kreuger of Uppsala University (Uppsala, Sweden) for helpful discussions. We are also grateful to Jon Deakin, Graham Rushton, Nijole Gasiunas and Patricia Hyde (Department of Medical Oncology, University of Manchester) and Susan Park (Harvard Medical School, Boston, MA, U.S.A.) for excellent technical advice and assistance. This work was supported by Cancer Research UK and Entremed Corp. (Boston, MA, U.S.A.). J. F. was supported by a grant from National Institutes of Health (Bethesda, MD, U.S.A.).

REFERENCES

1 Bernfield, M., Gotte, M., Park, P., Reizes, O., Fitzgerald, M., Lincecum, J. and Zako, M. (1999) Functions of cell surface heparan sulfate proteoglycans. Annu. Rev. Biochem. **68**, 729–777

2 Gallagher, J. and Lyon, M. (2000) Heparan sulphate: molecular structure and interactions with growth factors and morphogens. In Proteoglycans: Structure, Biology and Molecular Interactions (Iozzo, R., ed.), pp. 27–60, Marcel Dekker, New York

3 Lindahl, U., Kusche-Gullberg, M. and Kjellén, L. (1998) Regulated diversity of heparan sulfate. J. Biol. Chem. **273**, 24979–24982

4 O'Reilly, M. S., Boehm, T., Shing, Y., Fukai, N., Vasios, G., Lane, W. S., Flynn, E., Birkhead, J. R., Olsen, B. R. and Folkman, J. (1997) Endostatin: an endogenous inhibitor of angiogenesis and tumour growth. Cell (Cambridge, Mass.) **88**, 277–285

5 Dhanabal, M., Ramchandran, R., Waterman, M. J., Lu, H., Knebelmann, B., Segal, M. and Sukhatme, V. P. (1999) Endostatin induces endothelial cell apoptosis. J. Biol. Chem. **274**, 11721–11726

6 Yamaguchi, N., Anand-Apte, B., Lee, M., Sasaki, T., Fukai, N., Shapiro, R., Que, I., Lowik, C., Timpl, R. and Olsen, B. (1999) Endostatin inhibits VEGF-induced endothelial cell migration and tumor growth independently of zinc binding. EMBO J. **18**, 4414–4423

7 Karihaloo, A., Karumanchi, S., Barasch, J., Jha, V., Nickel, C., Yang, J., Grisaru, S., Bush, K., Nigam, S., Rosenblum, N. et al. (2001) Endostatin regulates branching morphogenesis of renal epithelial cells and ureteric bud. Proc. Natl. Acad. Sci. U.S.A. **98**, 12509–12514

8 Halfter, W., Dong, S., Schurer, B. and Cole, G. (1998) Collagen XVIII is a basement membrane heparan sulphate proteoglycan. J. Biol. Chem. **273**, 25404–25412

9 Hohenester, E., Sasaki, T., Olsen, B. and Timpl, R. (1998) Crystal structure of the angiogenesis inhibitor endostatin at 1.5 Å resolution. EMBO J. **17**, 1656–1664

10 Sasaki, T., Larsson, H., Kreuger, J., Salmivirta, M., Claesson-Welsh, L., Lindahl, U., Hohenester, E. and Timpl, R. (1999) Structural basis and potential role of heparin/heparan sulfate binding to the angiogenesis inhibitor endostatin. EMBO J. **18**, 6240–6248

11 Dixelius, J., Larsson, H., Sasaki, T., Holmqvist, K., Lu, L., Engstrom, A., Timpl, R., Welsh, M. and Claesson-Welsh, L. (2000) Endostatin-induced tyrosine kinase signaling through the Shb adaptor protein regulates endothelial cell apoptosis. Blood **95**, 3403–3411

12 Karumanchi, S., Jha, V., Ramchandran, R., Karihaloo, A., Tsiokas, L., Chan, B., Dhanabal, M., Hanai, J., Venkataraman, G., Shriver, Z. et al. (2001) Cell surface glypicans are low-affinity endostatin receptors. Mol. Cell **7**, 811–822

13 Kreuger, J., Matsumoto, T., Vanwildemeersch, M., Sasaki, T., Timpl, R., Claesson-Welsh, L., Spillman, D. and Lindahl, U. (2002) Role of heparan sulfate domain organization in endostatin inhibition of endothelial cell function. EMBO J. **21**, 6303–6311

14 Ding, Y. H., Javaherian, K., Lo, K. M., Chopra, R., Boehm, T., Lanciotti, J., Harris, B. A., Li, Y., Shapiro, R., Hohenester, E. et al. (1998) Zinc-dependent dimers observed in crystals of human endostatin. Proc. Natl. Acad. Sci. U.S.A. **95**, 10443–10448

15 Lo, K. M., Sudo, Y., Chen, J., Li, Y., Lan, Y., Kong, S. M., Chen, L., An, Q. and Gillies, S. D. (1998) High level expression and secretion of Fc-X fusion proteins in mammalian cells. Protein Eng. **11**, 495–500

16 Lyon, M., Rushton, G., Askari, J., Humphries, M. and Gallagher, J. (2000) Elucidation of the structural features of heparan sulfate important for interaction with the hep-2 domain of fibronectin. J. Biol. Chem. **275**, 4599–4606

17 Lyon, M., Deakin, J. A., Mizuno, K., Nakamura, T. and Gallagher, J. T. (1994) Interaction of hepatocyte growth factor with heparan sulfate. Elucidation of the major heparan sulfate structural determinants. J. Biol. Chem. **269**, 11216–11223

18 Merry, C. L. R., Lyon, M., Deakin, J. A., Hopwood, J. J. and Gallagher, J. T. (1999) Highly sensitive sequencing of the sulfated domains of heparan sulfate. J. Biol. Chem. **274**, 18455–18462

19 Merry, C. L. R., Bullock, S. L., Swan, D. C., Backen, A. C., Lyon, M., Beddington, R. S. P., Wilson, V. A. and Gallagher, J. T. (2001) The molecular phenotype of heparan sulfate in the *Hs2st*$^{-/-}$ mutant mouse. J. Biol. Chem. **276**, 35429–35434

20 Maccarana, M. and Lindahl, U. (1993) Mode of interaction between platelet factor 4 and heparin. Glycobiology **3**, 271–277

21 Wasteson, A. (1971) A method for the determination of the molecular weight and molecular weight distribution of chondroitin sulphate. J. Chromatogr. **59**, 87–97

22 Sasaki, T., Fukai, N., Mann, K., Gohring, W., Olsen, B. and Timpl, R. (1998) Structure, function and tissue forms of the C-terminal globular domain of collagen XVIII containing the angiogenesis inhibitor endostatin. EMBO J. **17**, 4249–4256

23 Turnbull, J. E. and Gallagher, J. T. (1991) Sequence analysis of heparan sulphate indicates defined location of N-sulphated glucosamine and iduronate 2-sulphate residues proximal to the protein-linkage region. Biochem. J. **277**, 297–303

24 Yamada, S., Yoshida, K., Sugiura, M., Sugahara, K., Khoo, K. H., Morris, H. R. and Dell, A. (1993) Structural studies on the bacterial lyase-resistant tetrasaccharides derived from the antithrombin III-binding site of porcine intestinal heparin. J. Biol. Chem. **268**, 4780–4787

25 Rice, K. G. and Linhardt, R. (1989) Study of structurally defined oligosaccharide substrates of heparin and heparan monosulphate lyases. Carbohydr. Res. **190**, 219–233

26 Salmivirta, M., Lidholt, K. and Lindahl, U. (1996) Heparan sulfate: a piece of information. FASEB J. **10**, 1270–1279

27 Turnbull, J. E., Fernig, D. G., Ke, Y., Wilkinson, M. C. and Gallagher, J. T. (1992) Identification of the basic fibroblast growth factor binding sequence in fibroblast heparan sulfate. J. Biol. Chem. **267**, 10337–10341

28 Taddei, L., Chiarugi, P., Brogelli, L., Cirri, P., Magnelli, L., Raugei, G., Ziche, M., Granger, H. J., Chiarugi, V. and Ramponi, G. (1999) Inhibitory effect of full-length human endostatin on *in vitro* angiogenesis. Biochem. Biophys. Res. Commun. **263**, 340–345

29 Pye, D., Vivés, R., Turnbull, J., Hyde, P. and Gallagher, J. (1998) Heparan sulfate oligosaccharides require 6-O-sulfation for promotion of basic fibroblast growth factor mitogenic activity. J. Biol. Chem. **273**, 22936–22942

Received 19 May 2003/12 June 2003; accepted 18 June 2003
Published as BJ Immediate Publication 18 June 2003, DOI 10.1042/BJ20030730